



# Progress of water desalination applications based on wettability and surface characteristics of graphene and graphene oxide: A review

Husam Hussein Ibrahim ELTIGANI<sup>1</sup>, Yuttanant BOONYONGMANEERAT<sup>2,\*</sup>

<sup>1</sup> Nanoscience and Technology Interdisciplinary Program, Graduate School, Chulalongkorn University, Pathumwan, Bangkok

<sup>2</sup> Metallurgy and Materials Science Research Institute, Chulalongkorn University, Pathumwan, Bangkok 10330, Thailand

\*Corresponding author e-mail: yuttanant.b@chula.ac.th

## Received date:

5 August 2022

## Revised date

29 August 2022

## Accepted date:

29 August 2022

## Keywords:

Desalination;  
Membranes;  
Graphene;  
Hydrophobicity;  
Hydrophilicity

## Abstract

Seawater desalination techniques have been continuously developed to tackle the water scarcity problems. This review article provides comprehensive discussion on the progress of water desalination applications that utilize the unique wettability and surface characteristics of graphene and graphene oxides, which are being employed as ultrafiltration membranes in either a monolayer or multilayer nanosheet configuration. The interaction of water with graphene materials and their wetting characteristics as well as the controlling factors are examined. Particularly, the designs and roles of hydrophilic and hydrophobic nanopores and nanochannels are discussed. A focus is also made on recent developments of graphene membrane with respect to water flow, salt rejection and durability.

## 1. Introduction

### 1.1 Application of graphene with water interaction

Graphene has found potential uses in a range of applications that require direct interaction between its surface and water molecules, owing to its unique physical and chemical characteristics that results in many beneficial functionalities, such as absorption, lubrication, surface condensation, separation and sensing. These include a wide range of applications, namely hydraulic power generation [1], water evaporation [2], water heat exchangers [3], nanofluids [4], water disinfection treatment [5], water desalination [6,7] and as biosensor [8]. Additionally, graphene oxide (GO) and reduced graphene oxide (rGO), which could be obtained respectively by oxidation of graphite and reduction of GO, have also been demonstrated to exhibit unique characteristics and add-on functionalities, such as the antimicrobial nature and thus anti-fouling properties. Therefore, they are also being explored for possibilities to use in the fields that require water interaction [9].

Water heat exchanger components whose surfaces are coated with graphene, for example, show good heat dissipation, high condensation rate, and corrosion protection, due to graphene's high specific area and stability [10]. In water and oil separation application, graphene, along with GO and rGO that are applied on a membrane surface provide unique oleophilicity and hydrophilicity leading to reduction of oil adhesion to the porous substrate and thus enhancement of water/oil separation efficiency [11-13]. Furthermore, due to its hydrophobic

characteristics, graphene-based coatings can be applied as anti-fouling agents on water surfaces to prevent adhesion of fouling and thus reducing the accumulation of marine-based deposits such as barnacles [14,15]

With increasingly high attentions in the research community recently, water desalination stands out as a promising application that utilizes the full benefit of graphene-based materials for sustainable developments for water resources. With their nano-porous feature and unique surface wettability function, graphene can serve as an ultrafiltration medium for chloride ions with frictionless solid-water interface that allows fast water transport [16]. In this review article, the recent advancement of graphene-based materials for water desalination applications will be reviewed and analyzed in detail.

### 1.2 Graphene desalination membranes

There are strong demands in many areas, especially those in water-stressed countries, for technological advancement of water desalination and thus the increase of water supply [17,18]. Because the typical desalination plant, based on heating and condensing seawater (multistage flash system (MSF)), requires large thermal and electric energy consumption [19], the alternative RO processes are developed whereby a semi-permeable nanofiltration membrane is employed to filter-out salt from saline water that is fed with high pressure [20]. Although the RO technology has been demonstrated to exhibit improved energy efficiency, low desalination capacity and low durability of membranes remain the issues, and thus the focus

has been addressed on the development of sturdy membranes with high water permeability, to be in place of the widely-used polyamide thin-film composite [21]. Particularly, a thin membrane layer (water flux is inversely proportional to membrane's thickness), high integrity (well-withstanding chloride and fouling attacks), and high-water permeability are among important characteristics for ideal membranes.

In this regard, graphene is considered a material of choice for ideal membranes because of its thin configuration and high chemical resistance [22]. Graphene can also be treated to form 2D nanochannels as permeable passages for water molecule [23]. Furthermore, graphene with and without functionalized atoms has unique wettability characteristics with water which can be further tailored to suit the application. Generally, there are 2 configurations of graphene-based desalination membranes, namely, a monolayer and multilayer type.

### 1.2.1 Monolayer graphene desalination membrane

Owing to a delocalized electronic cloud, pristine graphene with no porosity is highly impermeable to liquid and gases, even for helium with its molecular radius of 1.3 Å (Figure 1) [24]. A monolayer graphene desalination membrane thus consists of a single layer of graphene sheet and a distribution of nano-pores through which salt can be blocked and water molecules can flow through (Figure 2) [25]. Such nanopores can be formed by some techniques, such as oxygen plasma treatment and gallium ion bombardment. As exemplified in Figure 3, the oxygen plasma etching process can form a cluster of nanopores whose porosity can be controlled with exposure time [26].

With nanopores being formed on a graphene sheet, permeation of water molecules can be influenced by the inherent hydrophobia of the parent graphene, the wetting characteristic at the surface of the nanopores, and thus the developed capillary force that drives water transport [27]. As shown in Figure 4, nanopores can be functionalized as hydrogenated or hydroxylated pores. The hydrogenated pores, whose surface is hydrophobic, show good stability and can block salt well, but allow water molecules with a certain orientation to pass and thus provide a relative low flow rate [28]. On the other hand, hydrophilic hydroxylated pores facilitate water molecules to flow through as well as some salt ions.

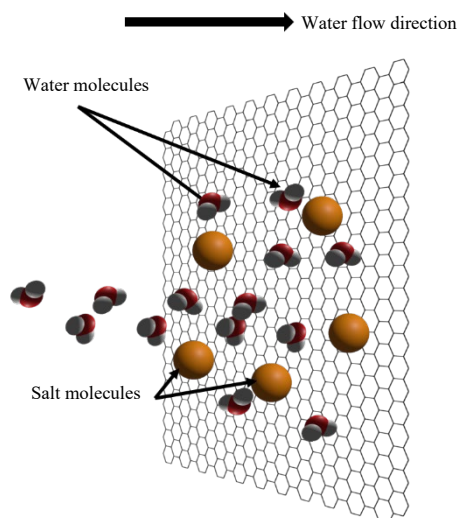


**Figure 1.** Impermeability of an ideal defect-free graphene sheet.

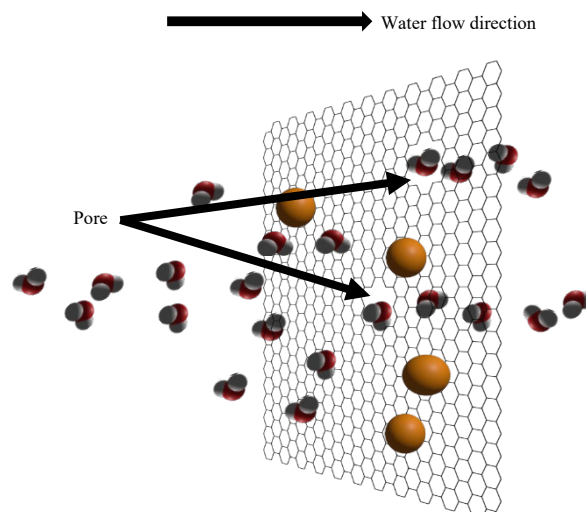


**Figure 2.** Water permeability of graphene sheet containing pores and obstruction of salt molecules.

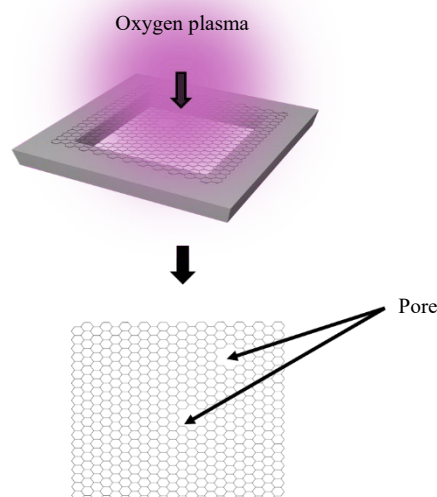


**Figure 3.** Oxygen plasma treatment for development of pores on a graphene sheet.

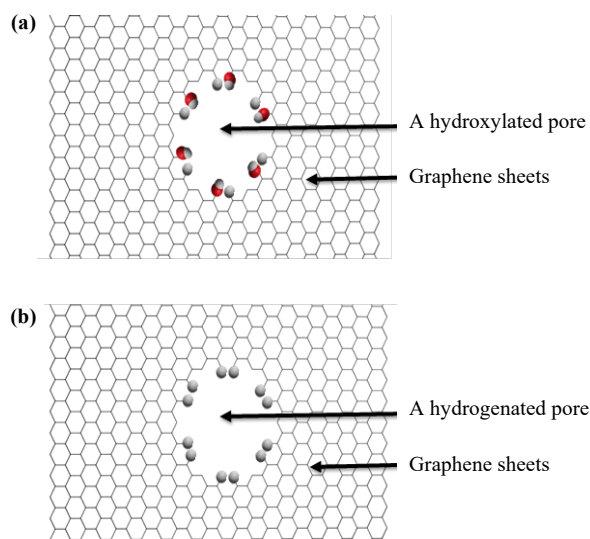


**Figure 4.** (a) hydroxylated pore (hydrophilic), (b) a hydrogenated pore (hydrophobic).

The study by Tanugi and Grossman [29] demonstrated that, with the optimum pore sizes for water permeation for the hydrophobic hydrogenated pores ( $23.1 \text{ \AA}^2$ ) and the hydrophilic hydroxylated pores ( $16.3 \text{ \AA}^2$ ), the two exhibited different water permeability from around  $39 \text{ L}\cdot\text{cm}^{-1}\cdot\text{day}^{-1}\cdot\text{Mpa}^{-1}$  to  $66 \text{ L}\cdot\text{cm}^{-1}\cdot\text{day}^{-1}\cdot\text{Mpa}^{-1}$  respectively. According to another study by Tanugi and Grossman [30], when pore size is enlarged from the optimum  $0.2 \text{ nm}$  to  $0.4 \text{ nm}$ , the salt rejection efficiency is found to drop to  $84\%$  and  $52\%$  respectively for the hydrophobic hydrogenated nanopores and hydrophilic hydroxylated nanopores. In addition, Xu *et al.* [31] found that the hydrophilic membranes with different contact angle ( $\text{CA} = 29^\circ, 50^\circ$ , or  $70^\circ$ ) have nearly zero pressure difference because the hydrophilic pores of the membranes could be constantly wet and no external pressure is needed. But for hydrophobic pore membranes, pressures rise rapidly with increasing the contact angle. Konatham *et al.* [32] examined the performance of using graphene sheets with different pores diameters ( $7.5 \text{ \AA}, 10.5 \text{ \AA}, 14.5 \text{ \AA}$ ) to exclude  $\text{Cl}^-$  from passing through the membrane. Their result showed that narrow graphene pores functionalized with hydroxyl groups remain effective for  $\text{Cl}^-$  ions. The work by Seongpil *et al.* [33] also confirms a higher water flux but lower salt rejection for hydrophilic pore membranes. However, it is important that the pore size is well-controlled such that the membranes can withstand the required high pressure of  $50 \text{ bar}$  to  $100 \text{ bar}$  during seawater desalination [34].

### 1.2.2 Multilayer graphene oxide desalination membrane

In the multilayer membrane configuration, graphene oxide (GO) nanosheets are stacked on one another via interlayer hydrogen bonds, as shown in Figure 5. This configuration, which could be produced by chemical oxidation, facilitates a fabrication of a relatively large and leak-free membrane. Between the stacked GO nanosheets present 2D nanochannels through which water can permeate while blocking salt. A GO nanosheet comprises of oxygen functional groups, such as hydroxyl and epoxy groups in the basal plane and carboxylic groups at the edges [34-36]. Overall, these features reflect in a moderately fast rate of water flow which can travel through planar nanochannels as well as open space between edges. This stems from the hydrophilic character of  $\text{OH}^-$  groups, which can form hydrogen-bond with water and provide smoother entropy for water molecule transport. Furthermore, frictionless flow of water takes place on the surface

of GO locally where graphene remained unoxidized [37]. It should be noted also that the wetting behavior of graphene oxide depends on the degree of oxidation.

Selectivity of ions is one of the main challenges for desalination design to provide water that is effectively free of salt [38,39]. The salt rejection efficiency can be improved by functionalizing the pores with oxygen-containing groups that have a high affinity for metals ions [40,41]. Spacing between the stacking GO is another important parameter for the barrier properties of the membrane. Typically, the interlayer space is  $0.83 \text{ nm}$ , which can be enlarged by increasing the degree of oxidation up to  $1 \text{ nm}$ , or decreased by reduction of GO [42]. Alternatively, hydrophobic nanopores, whose size ( $0.3 \text{ nm}$ ) is just nearly the diameter of water molecules ( $0.26 \text{ nm}$ ), can be induced on a plane of GO to improve the salt rejection rate [43]. Through reduction processes, GO can be converted to reduced GO (rGO), a graphene sheet with some residual oxygen and structural defects. Similar to GO, rGO can be considered for multilayer membranes. The static water contact angles of GO and rGO are  $\sim 34 \pm 2^\circ$  and  $\sim 76 \pm 5^\circ$ , respectively [44].

Comparison of graphene and graphene oxide-based membranes for water desalination applications is presented in Table 1.

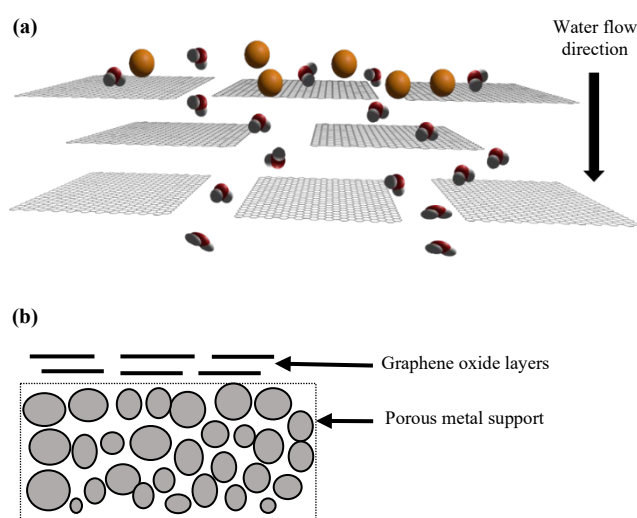


**Figure 5.** (a) Diffusion of water molecules through the channels of graphene oxide layers and rejection of salt, and (b) Graphene oxide layers on a porous metal support.

**Table 1.** Comparison of graphene and graphene oxide in water desalination application.

Features	Porous graphene membrane	Graphene oxide membrane
Molecule separation Performance	Excellent	Less performance
Durability / Mechanical stability	Good in case for resistance the water pressure	Unsatisfactory for practical application because of the unstable chemical structure/ reduced by the thinner sheets
Water flux	High with better selectively for salt ions	Restricted by the tortuosity (e.g twisted or have many turn) although thinner GOMs provide high water flux
Scalability	Poor and depend on the synthesis methods and handling	Good scalable
Water transport	Fast	Slow because of the prominent side pinning effect from capillaries formed around the oxidized region
Fabrication cost	Expensive	Considered cheaper than a porous graphene membrane according to the methodology and raw materials use (graphite)

## 2. Influential factors on the wettability of graphene

As discussed previously, wettability of graphene-based materials is an important influential factor that influences water flux in the water desalination membrane. The intrinsic wetting angle of pristine, isolated non-supported monolayer graphene is related to the surface energy of graphene ( $47.6 \text{ mJ}\cdot\text{m}^{-2}$ ) and of graphene oxide ( $61.2 \text{ mJ}\cdot\text{m}^{-2}$ ) [45]. Graphene, as one of the carbon-based materials, is also considered to be sensitive to the  $\text{sp}^2/\text{sp}^3$  bonding ratio on the surface [46]. However, its contact angle was found to be around  $90^\circ$  by many researchers [47,48] and recorded  $85^\circ \pm 5^\circ$  for partially suspended monolayer graphene on a nanopatterned silicon substrate [49]. In addition, the water molecules are oriented to hydrogen bond to make H- $\pi$  bonding with a single layer of graphene [50].

Wettability of graphene is controlled by several factors including the physical and chemical states of the materials themselves, the substrate upon which graphene is applied on, and environmental conditions, as follows:

### 2.1 Graphene

1) Type of graphene: GO and rGO exhibit hydrophilic, whereas pristine graphene is generally hydrophobic

2) Defects: Several types of defects, including wrinkle and ripple layers, line defects, and edge distortion, can be developed on graphene due to synthesis process or handling. Defects, such as wrinkles, can result in carbon-oxygen bonds which exhibit hydrophilic behavior when come to contact with water [51]. On the other hand, defects such as groove and triangle defects induce the pinning effect [52]. A summary of possible defects is tabulated in Table 2.

3) Number of layers: A single layer of graphene was tested to exhibit wetting transparency of an underlying substrate [53]. However, the increase of the number of graphene layers usually lead to water contact angle increment. This is because by increasing the layers, the influence of the underlying substrate becomes more negligible and therefore the most top layer of graphene can act independently [54].

### 2.2 Substrate

The wettability of graphene is largely controlled by the underlying substrates which by themselves exhibit various degree of wettability

depending on their surface energy [55]. Furthermore, surface polarity also leads to a higher degree of hydrophilicity. The contact angles for the substrates without and with monolayer graphene are as follows: Polyethylene Terephthalate (PET) ( $19.7^\circ/53.7^\circ$ ), Silicon ( $42.2^\circ/79.7^\circ$ ), Quartz ( $51.2^\circ/72.7^\circ$ ), Glass ( $52.2^\circ/76.5^\circ$ ), Copper ( $55.2^\circ/78.7^\circ$ ), 300 nm Silica/Silicon ( $65.7^\circ/80.2^\circ$ ), HF-Silicon ( $81.7^\circ/82.2^\circ$ ), PDMS ( $114^\circ/94.2^\circ$ ), Gold ( $77.4^\circ/78.8^\circ$ ) [56].

### 2.3 Environmental condition:

Rises of humidity [57] and temperature [58] usually increase the wettability of water on graphene, whereas absorption and accumulation of air contaminant usually increase the degree of hydrophobicity on graphene surface [59].

## 3. Recent research advancement

### 3.1 On porous graphene

#### 3.1.1 Improvement of water flow

Attempts are being made to increase the flow of water in many fronts. For example, a particular form of nano-porous graphene, so-called Holey-graphene (HG) [60], consisting of vertically separated arrangement of multilayers of nano-porous graphene, was numerically investigated. Graphene holes can trigger capillarity-driven inhibition to create an equilibrium wetting state and therefore enhanced graphene-water contact areas, hydrophilicity and hence water flow improvement. On the other hand, electric field may be applied to the membrane system to promote the micro/nanofluidic behavior of water leading to water flow enhancement [61,62]. Another interesting strategy is the integration of a multilayer nanoporous graphene NPG membrane with the smallest possible layer separation and fully aligned pores. With this design, hydraulic resistance across the membrane could be subdued. Depending on pore size, the permeability of using 200-layer nano pristine nanoporous graphene NPG membrane could be as high as approximately  $2 \text{ L}\cdot\text{m}^{-2}\cdot\text{h}^{-1}\cdot\text{bar}^{-1}$  [63]. A recent study on liquid transport through a nanoporous graphene membrane sheds more lights on how pore sizes affect pore center velocity and slip velocity, owing to van der waals forces [64].

**Table 2.** Possible defects of graphene and their causes.

Defects	Causes	Ref
Topological faults (Pentagon, heptagon)	Transform from $\text{sp}^2$ to $\text{sp}^3$	[106]
Geometric strain	Higher chemical reactivity or from Thermal Expansion Coefficient (TCE) mismatch between graphene ( $(-8.0 \pm 0.7) \times 10^{-6} \text{ K}^{-1}$ at room temperature) and a substrate	[106,107]
Zigzag edge distortion	Aromatic sextet (it can cause thermodynamic instability)	[108]
Ripples layer	Pore adhesion or interfacial instability	[109]
Wrinkle layer	Surface energy reduction; residual stress; thermal expansion mismatch between graphene and a substrate	[110]
Twisted-angle disorder	Two layers of graphene stacked on each other but with different angles coming from the non-formality of twisted bilayer graphene across a sample	[111]

### 3.1.2 Improvement of salt rejection

Promotion of salt rejection can be induced through many routes, ranging from designing of pore structures in the graphene membranes to ion functionalization and application of electric field. By developing sub-nanometer pores in graphene-based membranes through a unique method comprising reduction and carbonization of graphene oxide nanosheet and polymer on a porous ceramic substrate, Chen *et al.* [16] demonstrated a high salt rejection rate of 99.99% with flux enhancement up to about 61%. It is also suggested that by controlling graphene membranes' surface to be less hydrophobic, entering of water molecules, and thus good water permeability and salt rejection percentage will be promoted. The study by S.P. Surwade and co-workers [65] shows that oxygen plasma etching is an efficient tool to tune pore size and nanopore density of graphene membranes, and hence selectivity of the Na<sup>+</sup> and Cl<sup>-</sup> transports. Through a molecular dynamics (MD) simulation study, Fang *et al.* [66] showed that ionization of the functional groups along the perimeter of the nanopores in single-layer graphene oxide membranes can adversely affect desalination performance. Particularly, interactions of water molecules with the ionized functionalized groups, which may be generated by the operation conditions of the membrane such as the pH of the feed solution, can promote salt leakage and impact water transport. A. Lohrasebi and S. Rikhtehgaran [67], on the other hand, demonstrated with the MD simulations that by applying electric field onto a porous graphene membrane system, separation of positive and negative ions from salt-water can be well promoted, and thus desalination performance is greatly improved.

### 3.1.3 Improvement of the durability

It is known that pores tend to weaken a material by reducing its ultimate strength [68]. Although a support layer would add mechanical strength to the nanoporous graphene membrane, it still needs to be practically feasible. There is a possibility that graphene's hydrophobic behavior may be lost if it is exposed to salt water for over a month and continues to be subjected to high pressure. Some approaches have been established to increase the mechanical resistance. For example, Collin.M *et al.* [69] suggested using CO<sub>2</sub> laser processing instead of chemical modification alone to create durable super-hydrophobic graphene surfaces that offer a self-cleaning property. With CO<sub>2</sub> laser, it is possible to have low energy surfaces with suitable surface roughness. In addition, the relationship between porosity and modulus of elasticity in the case of nano-porosity must not be neglected while estimating the mechanical strength with the influence of porosity on the modulus of elasticity and the increasing elongation under shear stress. Some studies showed that the maximum pressure that nano-porous graphene can withstand depends not only on the size and spacing of the nanopores, but primarily on the radius of the pores in the substrate material [70]. At this point it should be mentioned that wrinkling phenomena became more evident with increasing elongation under shear stress. Therefore, strengthening the nanoporous graphene sheet is possible and can be achieved by controlling the porosity of graphene. It has been found that the fracture stress in graphene decreases with increasing porosity. In this study, the shear strain values at failure point were 0.397, 0.345, 0.3, 0.15, and

0.148 for porosity of 10.4%, 14.98%, 23.38%, 40%, and 50%, respectively [71].

## 3.2 On graphene oxide

### 3.2.1 Improvement of water flow

Effective improvement of water flux due to hydrophilicity of graphene oxide membranes can be achieved through several approaches. For example, doping with graphene oxide such as hydrophobic materials, such as polydimethylsiloxane PDMS, on a graphene membrane through amidation reaction is useful to control wettability [72]. This addition of PDMS (as hydrophobic material) was grafted onto the surface of GO films. It showed a higher degree of hydrophobicity (contact angle 129.5°) compared to GO-VF (vacuum filtration) membrane (80.5°). For better control of the water permeability, the interlayer spacing of GO membranes can be made below 10 Å by physical confinement such as epoxy encapsulant [73]. Another example is the case of using molybdenum disulfate MoS<sub>2</sub> with GO [74]. The hydrophilicity of this composite reported as 41.7° because there were many hydrophilic functional groups on the GO surface, but it became larger with increasing MoS<sub>2</sub> contents (55.9° to 65.5°). The advantage of MoS<sub>2</sub> in this composite was to resist the permeation of hydrophilic contaminants. Recent work showed that changing via size and shifted boundary have remarkable effects on water permeation between GO laminations, and water molecules can be adsorbed on the GO surface when molecules with high oxide groups are present. This is because an increase in the oxide concentration causes the flow channel to shrink, leading to more blockage events for water transport. Hu *et al.* [75] prepared piperazine (PIP) with GO by in situ interfacial polymerization of PIP-GO and trimesoyl chloride on a porous substrate, whereby GO induced a wrinkled membrane surface with increased roughness and hydrophilicity. This led to an improvement in water permeability, which is attributed to the increase in hydrophilicity due to the increase in surface area of the GO-PIP membranes. Moreover, Deng *et al.* [76] further improved membrane hydrophilicity, anti-fouling and chlorine resistance properties by adding SiO<sub>2</sub> nanoparticles. This additive SiO<sub>2</sub> creates a multitude of hydroxyl groups. Additionally, perforation strategies, such as photo-catalytic nanoporation, could lead to hybrid, highly permeable membranes. It was reported that the irradiation treatment influence water contact angles, membranes' structure, and hence improved water permeance [77].

### 3.2.2 Improvement of salt rejection

A low-cost, scalable partial combustion process of graphene oxide has been proposed to produce porous graphene with precise pore size control, which is expected to have high selectivity for K<sup>+</sup> and Na<sup>+</sup> ions with small pores [78]. With this process, most of the oxygen-containing groups can be removed from the GO upon firing. Salt rejection can reach 100% by using sub-nanometer pores as the only possible path for ions and water molecules [79]. Also use of a fabricated polyimide (PI)/graphene oxide (GO) mixed matrix membrane (MMM) with synthesized GO nanosheets was reported to have excellent salt rejection (99%) [80]. Through a molecular

dynamics (MD) simulation study, J. Zhang *et al.* [81] studied several factors that impact desalination performance. It was found that salt rejection is influenced largely by interlayer spacing. The distance between the layers arises from the large free energy between ions and graphene sheets and from a relatively large size of the hydration layer around the ions. Salt rejection values are close to 100% when interlayer spacing is 0.7 nm and 0.8 nm. In this method, the hydrophilic GO acted as a nucleating agent and accelerated membrane nucleation and growth and can therefore introduce an extended microporous finger-like structure and larger pore size. The presence of GO in the polymer solution can induce fast solvent/ non-solvent mass transfer due to the high hydrophilicity of GO. Zhang *et al.* [82] used typical inorganic ceramic tubes and polymeric polyacrylonitrile (PAN) and polycarbonate (PC) substrates to support GO membranes. This leads to water permeability of  $15.5 \text{ L}\cdot\text{m}^{-2}\cdot\text{h}^{-1}\cdot\text{bar}^{-1}$  and inorganic salts, including  $\text{Na}_2\text{SO}_4$ ,  $\text{NaCl}$ ,  $\text{MgSO}_4$ ,  $\text{MgCl}_2$  with 99.5% rejection, it was observed that salt rejection decreases at different rates with increasing salt concentration. In addition, Hu *et al.* [83] stated that GO membranes could not continuously reject salts ( $\text{Na}_2\text{SO}_4$ ,  $\text{NaCl}$ ,  $\text{KCl}$ ,  $\text{MgSO}_4$ , and  $\text{MgCl}_2$ ) over the long term under pressure-controlled conditions, indicating the lack of stable retention for GO membranes. In another work on improving water flux and salt rejection in membrane distillation, Xu *et al.* [84] reported an approach to fabricate a composite membrane by evaporation-assisted deposition of GO on a polyvinylidene difluoride (PVDF)/polydopamine (PDA) membrane. Salt rejection has been improved from 99.2% of the PVDF membrane to 99.9% for all composite membranes. In addition, the use of PDA improves the interfacial adhesion between the GO layer and the surface.

### 3.2.3 Improvement of durability

Manufacturing membranes that can exhibit mechanical and chemical robustness is most advantageous and in demand [85]. Building an ultra-thin and robust GO laminated membrane can be facilitated by blending GO with phenolic/polyether nanosheets [86]. Furthermore, a modified graphene oxide-functionalized chitosan (GO/f-Cs) membrane For more development, Du *et al.* [88] pointed out that after adding the silica nanoparticles to GO by in situ hydrolysis and vacuum suction filtration, oxide/silica (GO/SiO<sub>2</sub>) hybrid composite exhibited an increase in the contact angle from 42.4° to 80.7°. However, wrinkled structures were observed in this hybrid membrane due to the interaction between hydrophilic groups of nanosheets and the water drained under the nanosheets. In another attempt, the integration of pure GO- Laminate into a highly cross-linked polymer network (hydrophilic) can reduce anti-swelling behavior [89]. There is a similar investigation by using the film composite TFC with GO as hybrid composite TFC/GO membrane [90]. Without GO, the TFC membrane showed a sharp drop in salt rejection when the operating pressure was above 25 bar, as the mechanical stress on the membrane can lead to membrane deformation. However, with TFC/GO membranes, water flux increased when the operating pressure was increased from 7 bar to 35 bar, and the incorporation of GO into the membrane improved the mechanical stability of the membrane. Furthermore, Qian *et al.* [91] demonstrated the incorporation of graphene oxide (GO) into chitosan (CS) as chitosan has strong hydrophilicity. The

GO content on the surface not only increases hydrophobicity but also has a beneficial effect on mechanical strength due to the good compatibility of GO with chitosan. Alternatively, promotion of the stability of GO membranes has been demonstrated with the use of polydopamine (PDA) as a covalent linker of highly adhesive characteristics [43].

## 3.3 On reduced graphene oxide

### 3.3.1 Improvement of water flow

The water permeability of rGO membrane is typically low due to its hydrophobic behavior with contact angle greater than 83° compared to GO behavior [92] and in some works around 77° [93]. Also using a two-dimensional titanium dioxide monolayer (Ti<sub>0.87</sub>O<sub>2</sub>, simplified as TO nanosheets), it was investigated whether it intercalates into the GO layers under ultraviolet (UV) irradiation [94]. A simple vacuum filtration procedure was used and the use of irradiation resulted in the reduction of GO to rGO through the photocatalytic properties of TO. The hydrophilic conversion of the TO nanosheets within the laminates allows more water molecules to be adsorbed into and through the membranes. Many researchers have demonstrated approaches to obtain rapid water flux for rGO membranes. For example, rGO/TA (tannic acid) membrane showed much better hydrophilicity with contact angle around 26° than the GO membrane (~54°) [95]. In order to promote water permeation to be as high as GO, rGO is mainly treated with hydrophilic materials such as mixed cellulose ester MCE. The GO membrane formed on the MCE filter resulting in a light yellow membrane, and within 23 min the GO membrane turned black, indicating that GO was reduced to rGO [96]. Moreover, the possibility of controlling the reduction of GO nanosheets in different degrees by hydrothermal reduction methods has been reported [97] to improve water permeability with  $56.3 \text{ L}\cdot\text{m}^{-2}\cdot\text{h}^{-1}\cdot\text{bar}^{-1}$  (1 bar=0.1 MPa), with a high rejection rate of over 95%. For comparison, the GO membrane shows a hydrophilic surface with an average water contact angle of about 46°, but still retains the hydrophilic surface with a contact angle ranging from 76° to 88° at a heating temperature of 120°C and 180°C respectively during hydrothermal reduction. Furthermore, the development of uniform rGO membranes by mild H<sub>2</sub>O<sub>2</sub> oxidation was made by promoting planar nanopores in high density in GO membranes prior to vacuum filtration and thermal reduction of GO to rGO. These developed nanopores offer additional channels for water transport [98].

### 3.3.2 Improvement of salt rejection

The use of such rGO-incorporated membrane was reported to achieve over 99.97% salt rejection. Enhancing hydrophobicity via incorporation of rGO can help to repel salt-water solution. With based hydrophobic membrane such as hydrophobic poly-(vinylidene fluoride-co-hexafluoropropylene) (PVDF-HFP) for direct contact distillation application, the mixture of rGO and PVDF-HFP provides hydrophobic chains and can increase the water contact angle to around 139°. In this composite membrane approach, the salt rejection rate is calculated using the following equation:  $R = (C_f - C_p / C_f) \times 100\%$  where  $C_f$  is the feed concentration and  $C_p$  is the permeate concentration [99]. Even

under high water pressure with different pH values, rGO can structure stability through  $K^+$  modification [100]. In these rGO- $K^+$  membranes water permeability of  $86.1 \text{ L}\cdot\text{m}^{-2}\cdot\text{h}^{-1}\cdot\text{bar}^{-1}$  and a rejection rate of 99.8% of  $\text{FeCl}_3$  can be reached.  $K^+$  was chosen because they have smaller hydrated radii than other cations and the hydrated  $K^+$  can increase the hydrophilic interlayer spacing in the rGO- $K^+$  membrane. The  $K^+$  linked to the adjacent layers through the cation- $\pi$  interactions.

### 3.3.3 Improvement of durability

Both rGO and GO provide chemical endurance and shear resistance [101]. However, reduced graphene oxide rGO can outperform GO by using, for example, silver nanoparticles (nAg)@polydopamine (pDA) as a deposit on rGO. A pDA layer can be deposited on the rGO membranes by immersing them in an oxygen-rich dopamine solution ( $2 \text{ g}\cdot\text{L}^{-1}$ , pH 8.5). pDA is considered hydrophilic and offers good adhesion, a robust mechanical membrane, improves water permeability and reduces bacterial adhesion. This is because pDA contains many

hydrophilic functional groups such as catechol and amine [102]. It was also reported that the hydrophilicity of the rGO membranes was improved by increasing the concentration of rGO and  $\text{TiO}_2$  due to the presence of various hydrophilic and negatively charged functional groups on the rGO/ $\text{TiO}_2$  nanocomposite. The concentration ratio of 0.002 wt% to 0.03 wt% of rGO/ $\text{TiO}_2$  provided water contact angles of  $56.5^\circ$  to  $44.6^\circ$  [103]. In another example, the reduced graphene oxide with polyimide RGO-PI membrane was examined [104]. It has been demonstrated that this framework of RGO-PI membrane has high mechanical strength, and that when GO underwent thermal reduction to obtain rGO membrane, a dense layer with in-plane nanochannels/pores can be obtained. Enhancing of hydrophilicity of the rGO membranes by controlling parameters of oxygen plasma treatment has also been reported [105].

Table 3 illustrates the key performance and characteristics of some selected GO and rGO membranes that are promising and show interesting advancements.

**Table 3.** Performance and characteristics of GO and rGO-based water desalination membranes.

Membrane surfaces	Conditions	Permeate water flux ( $\text{L}\cdot\text{m}^{-2}\cdot\text{h}^{-1}$ )	Salt rejection (%)	Water contact angle ( $^\circ$ )	Ref.
GO vs. $\text{MoS}_2/\text{GO}$	GO dispersion ( $0.1 \text{ mg}\cdot\text{mL}^{-1}$ ), $\text{MoS}_2$ concentration (0.3, 0.6, 0.9 mL)	8.83-48.27	54.32-96.85	From $41.7^\circ$ to $55.9^\circ$ and continued to increase by increasing the $\text{MoS}_2$ contents until $65.5^\circ$	[74]
PI vs. PI/GO	Polyimide PI/GO concentration 0.9 wt%, pressure 15 (bar)	17.65 -26.05	84-98	From around 75 of pure PI to 68 when GO was incorporated	[80]
BW (TFC) vs. GO (f-Cs)/(PA)	NaCl solution ( $1500 \text{ mg}\cdot\text{mL}^{-1}$ , pH 7, $25^\circ\text{C}$ ), 14 Bar. commercial Brackish water BW thin fil composite (TFC) membrane	56.1- 61.5	88.7-95.6	From $63.68^\circ$ of unmodified membrane BW(TFC) to $19.13^\circ$ after GO / f-Cs) / PA coating	[87]
TFC vs. with GO coating	NaCl concentration is 2000 ppm, temperature $22^\circ\text{C}$ , pressure 15 (bar)	16.6-29.6	99-98	From $64^\circ$ of GO-free TFC to $49^\circ$ for TFC/GO	[90]
rGO)/TO (Titania)	$0.1 \text{ mg}\cdot\text{mL}^{-1}$ of GO- $0.08 \text{ mg}\cdot\text{mL}^{-1}$ of TO, 90 mL of a $0.1\text{-mol}\cdot\text{L}^{-1}$ salt solution and DI-water	$14.0 \pm 0.3$	$97.1 \pm 1.1$	Super hydrophilic Titania (TO) nanosheet can absorb more water	[94]
rGO/ $\text{TiO}_2$	rGO to $\text{TiO}_2$ molar ratio of 70:30, Concentration from 0.002 wt% to 0.03 wt.%, $2000 \text{ mg}\cdot\text{L}^{-1}$ NaCl solution	51.3	99.45	From $56.5^\circ$ to $44.6^\circ$ by increasing the concentration of rGO/ $\text{TiO}_2$	[103]
(rGO) vs. (GQDs/rGO)	GQDs graphene quantum dots, $1 \text{ g}\cdot\text{L}^{-1}$ of NaCl, 0.6 Mpa	16-31	75-65	Increased from $62.3^\circ$ of rGO to $71.9^\circ$ of defect-free structure of GQDs/rGO	[112]
GO-CA (cellulose acetate)	2000 Pam, pressure 30 (bar). GO concentration from 0 to 0.01 wt%	5.96-13.65	97.85-82.03	From $70.59^\circ$ to $53.42^\circ$ by increasing the concentration from 0 to 0.01 wt%	[113]
(PVDF-HFP) vs. (PVDF-HFP-rGO)	Vinylidene fluoride PVDF, hexafluoropropene HEP, $60 \text{ g}\cdot\text{L}^{-1}$ NaCl, pressure 34.4 kPa to 103.43 kPa	16.1-20.37	99.3-99.97	Increased from $\sim 123.5^\circ$ of PVDF-HFP to $\sim 139^\circ$ when rGO was incorporated	[99]
rGO-PTFE	Polytetrafluoroethylene (PTFE), Pressure 0.04 MPa, 3.5 wt% NaCl	68.3-65.7	98.5-98.2	Decreased from $150.3^\circ$ of pristine PTEF to $\sim 110.2^\circ$ of rGO-PTEF. rGO exhibit a robust structure.	[114]

#### 4. Conclusions

Graphene and graphene oxides are the promising medium being developed for ultrafiltration membranes for water desalination applications owing to their unique characteristics, including the 2D geometry, chemical stability, and surface wettability. Typically, the intrinsic wetting angle of graphene is around 90°, which in turn could be influenced by surface functionalization, defects, numbers of stacking layers, the underlined substrates, and environmental conditions. For a monolayer graphene membrane with nanopores that block salt and allow water to flow through, there are two configurations at present – with hydroxylated (hydrophilic) pores and with hydrogenated (hydrophobic) pores. The former shows fast transport, while the latter exhibits effective filtration. A stacking of graphene oxide nanosheets, on the other hand, allow production of large and leak-free membranes where water can transport at a fast rate through planar nanochannels and open space between edges. Degree of oxidation and interlayer spacing are among important parameters that determine their salt rejection rate. In the past 10 years, focuses have been placed on the development of the graphene membranes, including porous graphene, graphene oxide, and reduced graphene oxide, towards surface wettability enhancement and thus improvement of their desalination performance in terms of water flow, salt rejection, and durability.

#### Acknowledgements

The authors would like to pay special regards to Chulalongkorn 100th Anniversary scholarship for funding this work and to express sincere gratitude to Nanoscience and Nanotechnology program and Metallurgy and Materials Science Research Institute of Chulalongkorn University for continuous supports.

#### References

- [1] Y. Han, Z. Zhang, and L. Qu, "Power generation from graphene-water interactions," *FlatChem*, vol. 14, p. 100090, 2019.
- [2] H. T. Kieu, B. Liu, H. Zhang, K. Zhou, and A. W.-K. Law, "Molecular dynamics study of water evaporation enhancement through a capillary graphene bilayer with tunable hydrophilicity," *Applied Surface Science*, vol. 452, pp. 372-380, 2018.
- [3] R. Ranjbarzadeh, A. M. Isfahani, M. Afrand, A. Karimipour, and M. Hojaji, "An experimental study on heat transfer and pressure drop of water/graphene oxide nanofluid in a copper tube under air cross-flow: Applicable as a heat exchanger," *Applied Thermal Engineering*, vol. 125, pp. 69-79, 2017.
- [4] Q. Xie, M. A. Alibakhshi, S. Jiao, Z. Xu, M. Hempel, J. Kong, H. G. Park, and C. Duan, "Fast water transport in graphene nanofluidic channels," *Nature Nanotechnology*, vol. 13, no. 3, pp. 238-245, 2018.
- [5] B. Song, C. Zhang, G. Zeng, J. Gong, Y. Chang, and Y. Jiang, "Antibacterial properties and mechanism of graphene oxide-silver nanocomposites as bactericidal agents for water disinfection," *Archives of biochemistry and biophysics*, vol. 604, pp. 167-176, 2016.
- [6] A. Boretti, S. Al-Zubaidy, M. Vaclavikova, M. Al-Abri, S. Castelletto, and S. Mikhalovsky, "Outlook for graphene-based desalination membranes," *npj Clean Water*, vol. 1, no. 1, pp. 1-11, 2018.
- [7] V. Palmieri, F. Bugli, M. C. Lauriola, M. Cacaci, R. Torelli, G. Ciasca, C. Conti, M. Sanguinetti, M. Papi, and M. De Spirito, "Bacteria meet graphene: modulation of graphene oxide nanosheet interaction with human pathogens for effective antimicrobial therapy," *ACS Biomaterials Science & Engineering*, vol. 3, no. 4, pp. 619-627, 2017.
- [8] J. Peña-Bahamonde, H. N. Nguyen, S. K. Fanourakis, and D. F. Rodrigues, "Recent advances in graphene-based biosensor technology with applications in life sciences," *Journal of Nanobiotechnology*, vol. 16, no. 1, pp. 1-17, 2018.
- [9] A. Jayakumar, A. Surendranath, and P. Mohanan, "2D materials for next generation healthcare applications," *International Journal of Pharmaceutics*, vol. 551, no. 1-2, pp. 309-321, 2018.
- [10] J. Puértolas, M. Castro, J. Morris, R. Ríos, and A. Ansón-Casas, "Tribological and mechanical properties of graphene nanoplatelet/ PEEK composites," *Carbon*, vol. 141, pp. 107-122, 2019.
- [11] S. Yang, L. Chen, C. Wang, M. Rana, and P.-C. Ma, "Surface roughness induced superhydrophobicity of graphene foam for oil-water separation," *Journal of colloid and interface science*, vol. 508, pp. 254-262, 2017.
- [12] C.-J. Wu, Y.-F. Li, W.-Y. Woon, Y.-J. Sheng, and H.-K. Tsao, "Contact angle hysteresis on graphene surfaces and hysteresis-free behavior on oil-infused graphite surfaces," *Applied Surface Science*, vol. 385, pp. 153-161, 2016.
- [13] J. Chen, K. Li, H. Zhang, J. Liu, S. Wu, Q. Fan, and H. Xue, "Highly efficient and robust oil/water separation materials based on wire mesh coated by reduced graphene oxide," *Langmuir*, vol. 33, no. 38, pp. 9590-9597, 2017.
- [14] H. Jin, L. Tian, W. Bing, J. Zhao, and L. Ren, "Toward the application of graphene for combating marine biofouling," *Advanced Sustainable Systems*, vol. 5, no. 1, p. 2000076, 2021.
- [15] M. Muthu, J. Gopal, S. Chun, and S. K. Lee, "Hydrophobic bacteria-repellant graphene coatings from recycled pencil stubs," *Arabian Journal for Science and Engineering*, vol. 43, no. 1, pp. 241-249, 2018.
- [16] X. Chen, Y.-B. Zhu, H. Yu, J. Z. Liu, C. D. Easton, Z. Wang, Y. Hu, Z. Xie, H.-A. Wu, X. Zhang, D. Li, and H. Wang, "Ultrafast water evaporation through graphene membranes with subnanometer pores for desalination," *Journal of Membrane Science*, vol. 621, p. 118934, 2021.
- [17] M. Elimelech, and W. A. Phillip, "The future of seawater desalination: Energy, technology, and the environment," *Science*, vol. 333, no. 6043, pp. 712-717, 2011.
- [18] S. Burn, M. Hoang, D. Zarzo, F. Olewniak, E. Campos, B. Bolto, and O. Barron, "Desalination techniques—A review of the opportunities for desalination in agriculture," *Desalination*, vol. 364, pp. 2-16, 2015.
- [19] K. Reddy, and N. Ghaffour, "Overview of the cost of desalinated water and costing methodologies," *Desalination*, vol. 205, no. 1-3, pp. 340-353, 2007.



- [20] I. C. Karagiannis, and P. G. Soldatos, "Water desalination cost literature: review and assessment," *Desalination*, vol. 223, no. 1-3, pp. 448-456, 2008.
- [21] G.-R. Xu, J.-N. Wang, and C.-J. Li, "Strategies for improving the performance of the polyamide thin film composite (PA-TFC) reverse osmosis (RO) membranes: Surface modifications and nanoparticles incorporations," *Desalination*, vol. 328, pp. 83-100, 2013.
- [22] M. Bhuyan, S. Alam, M. Uddin, M. Islam, F. A. Bipasha, and S. S. Hossain, "Synthesis of graphene," *International Nano Letters*, vol. 6, no. 2, pp. 65-83, 2016.
- [23] G. Liu, W. Jin, and N. Xu, "Graphene-based membranes," *Chemical Society Reviews*, vol. 44, no. 15, pp. 5016-5030, 2015.
- [24] S. Homaeigohar, and M. Elbahri, "Graphene membranes for water desalination," *NPG Asia Materials*, vol. 9, no. 8, pp. e427-e427, 2017.
- [25] T. Humplik, J. Lee, S. O'Hern, B. A. Fellman, M. A. Baig, S. F. Hassan, M. A. Atieh, F. Rahman, T. Laoui, R. Karnik, and E. N. Wang, "Nanostructured materials for water desalination," *Nanotechnology*, vol. 22, no. 29, p. 292001, 2011.
- [26] A. Dey, A. Chronos, N. S. J. Braithwaite, R. P. Gandhiraman, and S. Krishnamurthy, "Plasma engineering of graphene," *Applied Physics Reviews*, vol. 3, no. 2, p. 021301, 2016.
- [27] Y. You, V. Sahajwalla, M. Yoshimura, and R. K. Joshi, "Graphene and graphene oxide for desalination," *Nanoscale*, vol. 8, no. 1, pp. 117-119, 2016.
- [28] E. N. Wang and R. Karnik, "Graphene cleans up water," *Nature nanotechnology*, vol. 7, no. 9, pp. 552-554, 2012.
- [29] D. Cohen-Tanugi and J. C. Grossman, "Water desalination across nanoporous graphene," *Nano letters*, vol. 12, no. 7, pp. 3602-3608, 2012.
- [30] D. Cohen-Tanugi and J. C. Grossman, "Nanoporous graphene as a reverse osmosis membrane: recent insights from theory and simulation," *Desalination*, vol. 366, pp. 59-70, 2015.
- [31] F. Xu, M. Wei, X. Zhang, Y. Song, W. Zhou, and Y. Wang, "How pore hydrophilicity influences water permeability?," *Research*, vol. 2019, 2019.
- [32] D. Konatham, J. Yu, T. A. Ho, and A. Striolo, "Simulation insights for graphene-based water desalination membranes," *Langmuir*, vol. 29, no. 38, pp. 11884-11897, 2013.
- [33] S. An, B. N. Joshi, J.-G. Lee, M. W. Lee, Y. I. Kim, M.-W. Kim, H. S. Jo, and S. S. Yoon, "A comprehensive review on wettability, desalination, and purification using graphene-based materials at water interfaces," *Catalysis Today*, vol. 295, pp. 14-25, 2017.
- [34] H. Huang, Y. Ying, and X. Peng, "Graphene oxide nanosheet: an emerging star material for novel separation membranes," *Journal of Materials Chemistry A*, vol. 2, no. 34, pp. 13772-13782, 2014.
- [35] P. Sun, M. Zhu, K. Wang, M. Zhong, J. Wei, A. Wu, Z. Xu, H. Zhu, "Selective ion penetration of graphene oxide membranes," *ACS nano*, vol. 7, no. 1, pp. 428-437, 2013.
- [36] F. Mouhat, F.-X. Coudert, and M.-L. Bocquet, "Structure and chemistry of graphene oxide in liquid water from first principles," *Nature communications*, vol. 11, no. 1, pp. 1-9, 2020.
- [37] Z. Zhang, L. Huang, Y. Wang, K. Yang, Y. Du, Y. Wang, M. J. Kipper, L. A. Belfiore, and J. Tang, "Theory and simulation developments of confined mass transport through graphene-based separation membranes," *Physical Chemistry Chemical Physics*, vol. 22, no. 11, pp. 6032-6057, 2020.
- [38] J. Choi, P. Dorji, H. K. Shon, and S. Hong, "Applications of capacitive deionization: Desalination, softening, selective removal, and energy efficiency," *Desalination*, vol. 449, pp. 118-130, 2019.
- [39] X. Zhou, Z. Wang, R. Epszten, C. Zhan, W. Li, J. D. Fortner, T. A. Pham, J.-H. Kim, and M. Elimelech, "Intrapore energy barriers govern ion transport and selectivity of desalination membranes," *Science advances*, vol. 6, no. 48, p. eabd9045, 2020.
- [40] E. Yang, C.-M. Kim, J.-h. Song, H. Ki, M.-H. Ham, and I. S. Kim, "Enhanced desalination performance of forward osmosis membranes based on reduced graphene oxide laminates coated with hydrophilic polydopamine," *Carbon*, vol. 117, pp. 293-300, 2017.
- [41] H.-H. Huang, R. K. Joshi, K. K. H. De Silva, R. Badam, and M. Yoshimura, "Fabrication of reduced graphene oxide membranes for water desalination," *Journal of Membrane Science*, vol. 572, pp. 12-19, 2019.
- [42] Y. Wei, Y. Zhang, X. Gao, Z. Ma, X. Wang, and C. Gao, "Multilayered graphene oxide membranes for water treatment: A review," *Carbon*, vol. 139, pp. 964-981, 2018.
- [43] K. Xu, B. Feng, C. Zhou, and A. Huang, "Synthesis of highly stable graphene oxide membranes on polydopamine functionalized supports for seawater desalination," *Chemical Engineering Science*, vol. 146, pp. 159-165, 2016.
- [44] B. Tang, L. Zhang, R. Li, J. Wu, M. N. Hedhili, and P. Wang, "Are vacuum-filtrated reduced graphene oxide membranes symmetric?," *Nanoscale*, vol. 8, no. 2, pp. 1108-1116, 2016.
- [45] S. Wang, Y. Zhang, N. Abidi, and L. Cabrales, "Wettability and surface free energy of graphene films," *Langmuir*, vol. 25, no. 18, pp. 11078-11081, 2009.
- [46] L. Y. Ostrovskaya, A. Dementiev, I. Kulakova, and V. Ralchenko, "Chemical state and wettability of ion-irradiated diamond surfaces," *Diamond and related materials*, vol. 14, no. 3-7, pp. 486-490, 2005.
- [47] X. Zhang, S. Wan, J. Pu, L. Wang, and X. Liu, "Highly hydrophobic and adhesive performance of graphene films," *Journal of Materials Chemistry*, vol. 21, no. 33, pp. 12251-12258, 2011.
- [48] J. Feng, and Z. Guo, "Wettability of graphene: from influencing factors and reversible conversions to potential applications," *Nanoscale Horizons*, vol. 4, no. 2, pp. 339-364, 2019.
- [49] T. Ondarçuhu, V. Thomas, M. Nunez, E. Dujardin, A. Rahman, C. T. Black, and A. Checco, "Wettability of partially suspended graphene," *Scientific reports*, vol. 6, no. 1, pp. 1-9, 2016.
- [50] E. Voloshina, D. Usvyat, M. Schütz, Y. Dedkov, and B. Paulus, "On the physisorption of water on graphene: a CCSD (T) study," *Physical Chemistry Chemical Physics*, vol. 13, no. 25, pp. 12041-12047, 2011.
- [51] R. Raj, S. C. Maroo, and E. N. Wang, "Wettability of graphene," *Nano letters*, vol. 13, no. 4, pp. 1509-1515, 2013.

- [52] S. K. Sethi, S. Kadian, and G. Manik, "A Review of recent progress in molecular dynamics and coarse-grain simulations assisted understanding of wettability," *Archives of Computational Methods in Engineering*, pp. 1-27, 2022.
- [53] J. Rafiee, X. Mi, H. Gullapalli, A. V. Thomas, F. Yavari, Y. Shi, P. M. Ajayan, and N. A. Koratkas, "Wetting transparency of graphene," *Nature materials*, vol. 11, no. 3, pp. 217-222, 2012.
- [54] J. Liu, C.-Y. Lai, Y.-Y. Zhang, M. Chiesa, and S. T. Pantelides, "Water wettability of graphene: interplay between the interfacial water structure and the electronic structure," *RSC advances*, vol. 8, no. 30, pp. 16918-16926, 2018.
- [55] F. Taherian, V. Marcon, N. F. van der Vegt, and F. Leroy, "What is the contact angle of water on graphene?," *Langmuir*, vol. 29, no. 5, pp. 1457-1465, 2013.
- [56] K. Xia, M. Jian, W. Zhang, and Y. Zhang, "Visualization of graphene on various substrates based on water wetting behavior," *Advanced Materials Interfaces*, vol. 3, no. 6, p. 1500674, 2016.
- [57] A. Qadir, Y. W. Sun, W. Liu, P. G. Oppenheimer, Y. Xu, C. J. Humphreys, and D. J. Dunstan, "Effect of humidity on the interlayer interaction of bilayer graphene," *Physical review B*, vol. 99, no. 4, p. 045402, 2019.
- [58] K. A. Emelyanenko, A. M. Emelyanenko, and L. B. Boinovich, "Water and ice adhesion to solid surfaces: Common and specific, the impact of temperature and surface wettability," *Coatings*, vol. 10, no. 7, p. 648, 2020.
- [59] Z. Li, Y. Wang, A. Kozbial, G. Shenoy, F. Zhou, R. McGinley, P. Ireland, B. Morganstein, A. Kunkel, S. P. Surwade, L. Li, and H. Liu, "Effect of airborne contaminants on the wettability of supported graphene and graphite," *Nature materials*, vol. 12, no. 10, pp. 925-931, 2013.
- [60] H. M. Hegab, P. Kallem, R. P. Pandey, M. Ouda, F. Banat, and S. W. Hasan, "Mechanistic Insights into the Selective Mass-transport and Fabrication of Holey Graphene-based Membranes for Water Purification Applications," *Chemical Engineering Journal*, p. 134248, 2021.
- [61] P. Jibin, S. Wan, Z. Lu, G. Zhang, and L. Wang "Controlled water adhesion and electrowetting of conducting hydrophobic graphene/carbon nanotubes composite films on engineering materials," *Journal of Materials Chemistry A*, vol. 1, no. 4, pp. 1254-1260, 2013.
- [62] M. Kargar, F. Khashei Varnamkhashti, and A. Lohrasebi, "Influence of electric fields on the efficiency of multilayer graphene membrane," *Journal of Molecular Modeling*, vol. 24, no. 9, pp. 1-8, 2018.
- [63] D. Cohen-Tanugi, L.-C. Lin, and J. C. Grossman, "Multilayer nanoporous graphene membranes for water desalination," *Nano letters*, vol. 16, no. 2, pp. 1027-1033, 2016.
- [64] J. A. Hossain, and B. Kim, "Scale effect on simple liquid transport through a nanoporous graphene membrane," *Langmuir*, vol. 37, no. 21, pp. 6498-6509, 2021.
- [65] S. P. Surwade, S. N. Smirnov, I. V. Vassiouk, R. R. Unocic, G. M. Veith, S. Dai, and S. M. Mahurin, "Water desalination using nanoporous single-layer graphene," *Nature nanotechnology*, vol. 10, no. 5, pp. 459-464, 2015.
- [66] C. Fang, Z. Yu, and R. Qiao, "Impact of surface ionization on water transport and salt leakage through graphene oxide membranes," *The Journal of Physical Chemistry C*, vol. 121, no. 24, pp. 13412-13420, 2017.
- [67] A. Lohrasebi and S. Rikhtehgaran, "Ion separation and water purification by applying external electric field on porous graphene membrane," *Nano Research*, vol. 11, no. 4, pp. 2229-2236, 2018.
- [68] W. C. Young, R. G. Budynas, and A. M. Sadegh, *Roark's formulas for stress and strain*. McGraw-Hill Education, 2012.
- [69] C. M. Tittle, D. Yilman, M. A. Pope, and C. J. Backhouse, "Robust superhydrophobic laser-induced graphene for desalination applications," *Advanced Materials Technologies*, vol. 3, no. 2, p. 1700207, 2018.
- [70] D. Cohen-Tanugi, and J. C. Grossman, "Mechanical strength of nanoporous graphene as a desalination membrane," *Nano letters*, vol. 14, no. 11, pp. 6171-6178, 2014.
- [71] T.-H. Fang, Z.-W. Lee, and W.-J. Chang, "Molecular dynamics study of the shear strength and fracture behavior of nanoporous graphene membranes," *Current Applied Physics*, vol. 17, no. 10, pp. 1323-1328, 2017.
- [72] W.-W. Lei, H. Li, L.-Y. Shi, Y.-F. Diao, Y.-L. Zhang, R. R. and W. Ni, "Achieving enhanced hydrophobicity of graphene membranes by covalent modification with polydimethylsiloxane," *Applied Surface Science*, vol. 404, pp. 230-237, 2017.
- [73] J. Abraham, J. Abraham, K. S. Vasu, C. D. Williams, K. Gopinadhan, Y. Su, C. T. Cherian, J. Dix, E. Prestat, S. J. Haigh, I. V. Grigorieva, P. Carbone, A. K. Geim, and R. R. Nair, "Tunable sieving of ions using graphene oxide membranes," *Nature nanotechnology*, vol. 12, no. 6, pp. 546-550, 2017.
- [74] J. Ma, X. Tang, Y. He, Y. Fan, and J. Chen, "Robust stable MoS<sub>2</sub>/GO filtration membrane for effective removal of dyes and salts from water with enhanced permeability," *Desalination*, vol. 480, p. 114328, 2020.
- [75] R. Hu, Y. He, C. Zhang, R. Zhang, J. Li, and H. Zhu, "Graphene oxide-embedded polyamide nanofiltration membranes for selective ion separation," *Journal of Materials Chemistry A*, vol. 5, no. 48, pp. 25632-25640, 2017.
- [76] H. Deng, Q. Zheng, H. Chen, J. Huang, J. Yan, M. Ma, M. Xia, K. Pei, H. Ni, and P. Ye, "Graphene oxide/silica composite nanofiltration membrane: Adjustment of the channel of water permeation," *Separation and Purification Technology*, vol. 278, p. 119440, 2021.
- [77] A. Guirguis, L. F. Dumée, X. Chen, L. Kong, H. Wang, and L. C. Henderson, "Photocatalytic-triggered nanopores across multilayer graphene for high-permeation membranes," *Chemical Engineering Journal*, vol. 443, p. 136253, 2022.
- [78] Z. Li, X. Zhang, H. Tan, W. Qi, L. Wang, M. C. Ali, H. Zhang, J. Chen, P. Hu, C. Fan, and H. Qiu, "Combustion fabrication of nanoporous graphene for ionic separation membranes," *Advanced Functional Materials*, vol. 28, no. 43, p. 1805026, 2018.
- [79] H. W. Kim, H. W. Yoon, S.-M. Yoon, B. M. Yoo, B. K. Ahn, Y. H. Cho, H. J. Shin, H. Yang, U. Paik, S. Kwon, J. H. Choi, and H. B. Park, "Selective gas transport through few-layered graphene and graphene oxide membranes," *Science*, vol. 342, no. 6154, pp. 91-95, 2013.
- [80] N. K. Zaman, R. Rohani, A. W. Mohammad, and A. M. Isloor, "Polyimide-graphene oxide nanofiltration membrane:

- Characterizations and application in enhanced high concentration salt removal," *Chemical Engineering Science*, vol. 177, pp. 218-233, 2018.
- [81] J. Zhang, C. Chen, J. Pan, L. Zhang, L. Liang, Z. Kong, X. Wang, W. Zhang, and J.-W. Shen, "Atomistic insights into the separation mechanism of multilayer graphene membranes for water desalination," *Physical Chemistry Chemical Physics*, vol. 22, no. 14, pp. 7224-7233, 2020.
- [82] M. Zhang, J. Sun, Y. Mao, G. Liu, and W. Jin, "Effect of substrate on formation and nanofiltration performance of graphene oxide membranes," *Journal of Membrane Science*, vol. 574, pp. 196-204, 2019.
- [83] R. Hu, G. Zhao, Y. He, and H. Zhu, "The application feasibility of graphene oxide membranes for pressure-driven desalination in a dead-end flow system," *Desalination*, vol. 477, p. 114271, 2020.
- [84] Z. Xu, X. Yan, Z. Du, J. Li, and F. Cheng, "Effect of oxygenic groups on desalination performance improvement of graphene oxide-based membrane in membrane distillation," *Separation and Purification Technology*, vol. 251, p. 117304, 2020.
- [85] W.-H. Zhang, M. J. Yin, Q. Zhao, C.-G. Jin, N. Wang, S. Ji, C. L. Ritt, M. Elimelech, and Q.-F. An, "Graphene oxide membranes with stable porous structure for ultrafast water transport," *Nature Nanotechnology*, vol. 16, no. 3, pp. 337-343, 2021.
- [86] Q. Lan, C. Feng, Z. Wang, L. Li, Y. Wang, and T. Liu, "Chemically laminating graphene oxide nanosheets with phenolic nanomeshes for robust membranes with fast desalination," *Nano Letters*, vol. 21, no. 19, pp. 8236-8243, 2021.
- [87] H. M. Hegab, Y. Wimalasiri, M. Ginic-Markovic, and L. Zou, "Improving the fouling resistance of brackish water membranes via surface modification with graphene oxide functionalized chitosan," *Desalination*, vol. 365, pp. 99-107, 2015.
- [88] Y.-C. Du, L.-J. Huang, Y.-X. Wang, K. Yang, Z.-J. Zhang, Y. Wang, M. J. Kipper, L. A. Belfiore, and J.-G. Tang, "Preparation of graphene oxide/silica hybrid composite membranes and performance studies in water treatment," *Journal of Materials Science*, vol. 55, no. 25, pp. 11188-11202, 2020.
- [89] S. Kim, R. Ou, Y. Hu, X. Li, H. Zhang, G. P. Simon, and H. Wang, "Non-swelling graphene oxide-polymer nanocomposite membrane for reverse osmosis desalination," *Journal of Membrane Science*, vol. 562, pp. 47-55, 2018.
- [90] M. E. Ali, L. Wang, X. Wang, and X. Feng, "Thin film composite membranes embedded with graphene oxide for water desalination," *Desalination*, vol. 386, pp. 67-76, 2016.
- [91] X. Qian, N. Li, Q. Wang, and S. Ji, "Chitosan/graphene oxide mixed matrix membrane with enhanced water permeability for high-salinity water desalination by pervaporation," *Desalination*, vol. 438, pp. 83-96, 2018.
- [92] Y. Wang, C. Wang, X. Song, S. K. Megarajan, and H. Jiang, "A facile nanocomposite strategy to fabricate a rGO-MWCNT photothermal layer for efficient water evaporation," *Journal of Materials Chemistry A*, vol. 6, no. 3, pp. 963-971, 2018.
- [93] L. Huang, J. Pei, H. Jiang, and X. Hu, "Water desalination under one sun using graphene-based material modified PTFE membrane," *Desalination*, vol. 442, pp. 1-7, 2018.
- [94] P. Sun, Q. Chen, X. Li, H. Liu, K. Wang, M. Zhong, J. Wei, D. Wu, R. Ma, T. Sasaki, and H. Zhu, "Highly efficient quasi-static water desalination using monolayer graphene oxide/titania hybrid laminates," *NPG Asia Materials*, vol. 7, no. 2, pp. e162-e162, 2015.
- [95] K. H. Thebo, X. Qian, Q. Zhang, L. Chen, H.-M. Cheng, and W. Ren, "Highly stable graphene-oxide-based membranes with superior permeability," *Nature communications*, vol. 9, no. 1, pp. 1-8, 2018.
- [96] H. Liu, H. Wang, and X. Zhang, "Facile fabrication of freestanding ultrathin reduced graphene oxide membranes for water purification," *Advanced materials*, vol. 27, no. 2, pp. 249-254, 2015.
- [97] Q. Zhang, X. Qian, K. H. Thebo, H.-M. Cheng, and W. Ren, "Controlling reduction degree of graphene oxide membranes for improved water permeance," *Science bulletin*, vol. 63, no. 12, pp. 788-794, 2018.
- [98] Y. Li, W. Zhao, M. Weyland, S. Yaun, Y. Xia, H. Liu, M. Jian, J. Yang, C. D. Easton, C. Selomulya, and X. Zhang, "Thermally reduced nanoporous graphene oxide membrane for desalination," *Environmental science & technology*, vol. 53, no. 14, pp. 8314-8323, 2019.
- [99] T. Chen, A. Soroush, and M. S. Rahaman, "Highly hydrophobic electrospun reduced graphene oxide/poly (vinylidene fluoride-co-hexafluoropropylene) membranes for use in membrane distillation," *Industrial & Engineering Chemistry Research*, vol. 57, no. 43, pp. 14535-14543, 2018.
- [100] R. Yang, Y. Fan, R. Yu, F. Dai, J. Lan, Z. Wang, J. Chen, and L. Chen, "Robust reduced graphene oxide membranes with high water permeance enhanced by K<sup>+</sup> modification," *Journal of Membrane Science*, vol. 635, p. 119437, 2021.
- [101] Z. Wang, F. He, J. Guo, S. Peng, X. Q. Cheng, Y. Zhang, E. Drioli, A. Figoli, Y. Li, and L. Shao, "The stability of a graphene oxide (GO) nanofiltration (NF) membrane in an aqueous environment: Progress and challenges," *Materials Advances*, vol. 1, no. 4, pp. 554-568, 2020.
- [102] E. Yang, A. B. Alayande, C.-M. Kim, J.-h. Song, and I. S. Kim, "Laminar reduced graphene oxide membrane modified with silver nanoparticle-polydopamine for water/ion separation and biofouling resistance enhancement," *Desalination*, vol. 426, pp. 21-31, 2018.
- [103] M. Safarpour, A. Khataee, and V. Vatanpour, "Thin film nanocomposite reverse osmosis membrane modified by reduced graphene oxide/TiO<sub>2</sub> with improved desalination performance," *Journal of Membrane Science*, vol. 489, pp. 43-54, 2015.
- [104] Z. Zhao, S. Ni, X. Su, Y. Gao, and X. Sun, "Thermally reduced graphene oxide membrane with ultrahigh rejection of metal ions' separation from water," *ACS Sustainable Chemistry & Engineering*, vol. 7, no. 17, pp. 14874-14882, 2019.
- [105] W. L. Xu, F. Zhou, and M. Yu, "Tuning water nanofiltration performance of few-layered, reduced graphene oxide membranes by oxygen plasma," *Industrial & Engineering Chemistry Research*, vol. 57, no. 47, pp. 16103-16109, 2018.
- [106] E. Celasco, A. Chaika, T. Stauber, M. Zhang, C. Ozkan, U. Ozkan, B. Palys, and S. W. Harun, "Handbook of graphene," 2019.

- [107] D. Yoon, Y.-W. Son, and H. Cheong, "Negative thermal expansion coefficient of graphene measured by Raman spectroscopy," *Nano letters*, vol. 11, no. 8, pp. 3227-3231, 2011.
- [108] J. Zhang, M. Terrones, C. R. Park, R. Mukherjee, M. Monthieux, N. Koratkar, Y. S. Kim, R. Hurt, E. Frackowiak, T. Enoki, Y. Chen, Y. Chen, A. Bianco, "Carbon science in 2016: Status, challenges and perspectives," *Carbon*, vol. 98, no. 70, pp. 708-732, 2016.
- [109] T. M. Paronyan, E. M. Pigos, G. Chen, and A. R. Harutyunyan, "Formation of ripples in graphene as a result of interfacial instabilities," *ACS nano*, vol. 5, no. 12, pp. 9619-9627, 2011.
- [110] A. Mohapatra, S. Das, K. Majumdar, M. R. Rao, and M. Jaiswal, "Thermal transport across wrinkles in few-layer graphene stacks," *Nanoscale Advances*, vol. 3, no. 6, pp. 1708-1716, 2021.
- [111] J. H. Wilson, Y. Fu, S. D. Sarma, and J. Pixley, "Disorder in twisted bilayer graphene," *Physical Review Research*, vol. 2, no. 2, p. 023325, 2020.
- [112] S. Yuan, Y. Li, R. Qiu, Y. Xia, C. Selomulya, and X. Zhang, "Minimising non-selective defects in ultrathin reduced graphene oxide membranes with graphene quantum dots for enhanced water and NaCl separation," *Chinese Journal of Chemical Engineering*, vol. 41, pp. 278-285, 2022.
- [113] Y. Shi, C. Li, D. He, L. Shen, and N. Bao, "Preparation of graphene oxide-cellulose acetate nanocomposite membrane for high-flux desalination," *Journal of Materials Science*, vol. 52, no. 22, pp. 13296-13306, 2017.
- [114] Y. Jia, G. Xu, X. An, and Y. Hu, "Robust reduced graphene oxide composite membranes for enhanced anti-wetting property in membrane distillation," *Desalination*, vol. 526, p. 115549, 2022.